IEEE Access
Multidisciplinary | Rapid Review | Open Access Journal

Received 4 July 2023, accepted 15 July 2023, date of publication 24 July 2023, date of current version 1 August 2023.

Digital Object Identifier 10.1109/ACCESS.2023.3298109

RESEARCH ARTICLE

A Novel Approach to Simultaneous Phonocardiography and Electrocardiography During Auscultation

SOFIA M. MONTEIRO AND HUGO PLÁCIDO DA SILVA, (Senior Member, IEEE)
Department of Bioengineering (DBE), Instituto Superior Técnico (IST), 1049-001 Lisbon, Portugal
Instituto de Telecomunicações (IT), 1049-001 Lisbon, Portugal

Corresponding author: Sofia M. Monteiro (sofia.m.monteiro@tecnico.ulisboa.pt)

This work was supported in part by Fundação para a Ciência e Tecnologia (FCT)/Ministério da Ciência, Tecnologia e Ensino Superior (MCTES) through National Funds and Co-Funded by European Union (EU) Funds under Project UIDB/50008/2020; and in part by FCT under Project DSAIPA/AI/0122/2020 (AIMHealth) and Project PCIF/SSO/0163/2019 (SafeFire).

This work involved human subjects or animals in its research. Approval of all ethical and experimental procedures and protocols was granted by the Ethics Committee of Instituto Superior Técnico under Statement No. 4/2023, and performed in line with the Declaration of Helsinki.

ABSTRACT The combination of the phonocardiogram (PCG) and the electrocardiogram (ECG) allows the simultaneous evaluation of the heart's mechanical and electrical conditions and could significantly improve the accuracy of an initial cardiovascular disease diagnosis. Both signals can be acquired using non-invasive and low-complexity devices. However, the currently available devices do not have a suitable form factor for the established medical routines, restricting their usability in clinical practice. They are also bound to proprietary tools that limit collaboration, which are constraints for both clinicians and researchers. To tackle these problems, we propose a novel electronic stethoscope that combines PCG and ECG sensors which use polymer-based dry electrodes with a previously validated 3D-printed acoustic stethoscope. We performed an experimental evaluation of the sensors, and the temporal relation between the two signals and heartbeat morphology were assessed. The effect of the rotation of the stethoscope head at different angles was also studied, further extending the state-of-the-art in the field. It was verified that the ECG lead voltages at different angles follow Kirchhoff's law, similar to the Einthoven leads. By comparing the ECG waveforms between a reference and the experimental device, the best case reached a Pearson's correlation coefficient of 0.916 ± 0.008. The results demonstrate the validity of the proposed electronic stethoscope, establishing a foundation for further development. The accessibility, low cost, and simplicity of the device should significantly facilitate its integration into healthcare facilities and telemedicine interventions, as well as into research and education.

INDEX TERMS Auscultation, electrocardiogram, electronic stethoscope, multimodal signals, phonocardiogram.

I. INTRODUCTION

Cardiovascular diseases (CVDs) are the leading cause of death globally and one of the main causes of increased morbidity, which lowers the quality of life of the patients and leads to incremental long-term healthcare costs. An early diagnosis of both congenital and acquired heart conditions, together with regular cardiac monitoring, is essential to reduce their burden and prevent premature deaths [1].

Techniques such as Computed Tomography (CT), Magnetic Resonance Imaging (MRI), and echocardiography can provide high-quality images and a detailed characterization of both the physiologic function and anatomy of the heart. However, these are inadequate for a first line of screening,

The associate editor coordinating the review of this manuscript and approving it for publication was Md. Kafiul Islam.

since they have a very high cost, requiring complex instrumentation and specialized personnel [2]. Additionally, they are typically only affordable in large hospitals in high-income countries, whereas, according to the World Health Organization (WHO), low- and middle-income countries have the highest prevalence of CVDs [3].

Even with the development of more advanced cardiac imaging exams, cardiac auscultation remains the most common primary screening method [4]. It is very straightforward, quick, and inexpensive, and by listening to the heart sounds doctors can diagnose several cardiac disorders related to the mechanical condition of the heart [5].

The time series of the heart sounds recording is named Phonocardiogram (PCG). It can be easily acquired with a microphone applied to the chest and then digitized for further analysis and processing [3]. Digital stethoscopes, which can record and store PCG signals during the auscultation routine, are paving the way for the development of automatic disease screening systems.

The ECG records the electrical activity of the heart and is also one of the most common primary disease screening methods. It is used to evaluate the heart's electrical condition and it is a very powerful, non-invasive, inexpensive, and easy-to-use technique. The ECG and the PCG are concurrent phenomena, seeing that the PCG results from the mechanical operation of the heart, which in turn relies on its electrical activation [6]. Thus, their simultaneous acquisition and analysis come as a natural step.

The potential of combining the two modalities has prompted the development of medical devices for the acquisition of synchronous PCG and ECG, enabled in part by recent developments in mobile health and telemonitoring [7]. Current devices are mostly based on integrating ECG electrodes in the head of an electronic stethoscope so the two signals can be acquired at the same time. One example is the Eko DUO system [8], [9], which records a single-lead ECG using two stainless steel electrodes attached to a rectangular stethoscope head. Another example is the CardioSleeve, which works as an add-on device to acoustic stethoscopes and enables the recording of the heart sounds and a 3-lead ECG [10], [11].

Other devices can also be found in the literature, such as the SmartHeart device, which integrated custom ECG electrodes on the diaphragm of the 3M Littmann 3200 to enable the simultaneous acquisition of the ECG and the PCG [12]. However, these devices still present several limitations, which have prevented their widespread implementation in clinical practice: their form factor is very different from the one of acoustic stethoscopes, which makes it difficult for doctors to use them in standard medical practices; the ECG leads that are acquired along the standard auscultation points are poorly characterized [12]; and they rely on proprietary software and hardware, which hinders collaboration and the sharing of the technology for use in research (where access to these devices is increasingly limited).

In this work, we present a novel device for simultaneous electrocardiography and phonocardiography during auscultation. It can perform a non-invasive assessment of the electrical and mechanical conditions of the heart and further contributes to the state-of-the-art by presenting a low-cost design that replicates the established form factor of standard analog stethoscopes. This work also includes an experimental evaluation of the device and sensors that addresses multiple practical aspects, such as the frequency response of the stethoscope, the concurrence between the two signals, and the effect of the rotation of the stethoscope head in the acquired ECG leads.

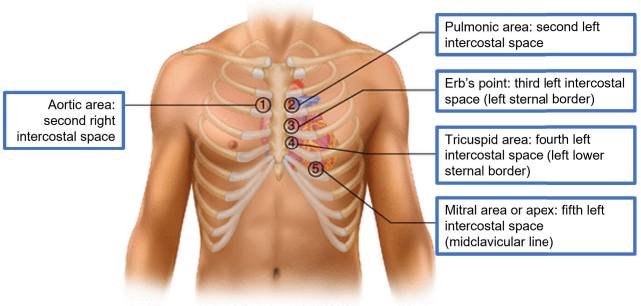

FIGURE 1. Five main cardiac auscultation points. Image from [14].

A. BACKGROUND

1) PHONOCARDIOGRAPHY (PCG)

In a PCG, the first heart sound (S1) and the second heart sound (S2) can always be identified. S1 results from the closing of the mitral and tricuspid valves and marks the beginning of ventricular systole, while S2 results from the closing of the aortic and pulmonary valves and marks the beginning of diastole [13]. These are called the fundamental heart sounds and produce the characteristic *lub-dub* sounds that are always audible during auscultation, with S1 forming the *lub* and S2, which is generally louder, shorter, and sharper than S1, forming the *dub*.

The third heart sound (S3) and the fourth heart sound (S4) are only present in some cases. They are very low sounds (typically with frequencies ranging from 20 to 70 Hz [15]) that appear, respectively, during early and late diastole, and can be indicators of pathology. It is also possible to observe clicks or heart murmurs, which result from turbulent blood flow and can have very different morphologies [13]. Placing the stethoscope at the different points of auscultation (Fig. 1), which are correlated with the location of the different cardiac valves, highlights the heart sounds or murmurs associated with those valves. This differential attenuation or enhancement of the heart sounds can be used to diagnose several valve diseases.

2) ELECTROCARDIOGRAPHY (ECG)

The ECG waveform results from a series of coordinated electrical events across the specialized conduction system of the heart. Any disturbance in this regular rhythmic activity can be a sign of pathology; as such, the ECG is extremely

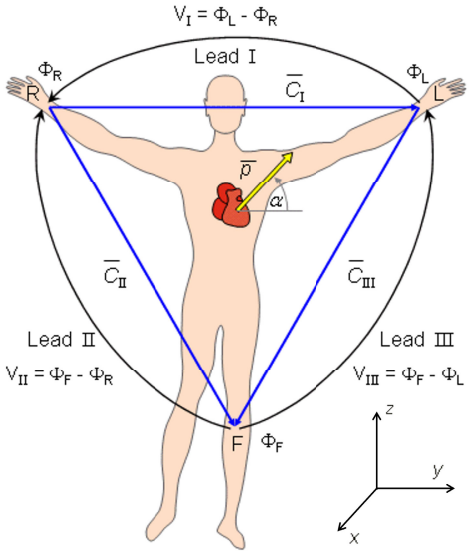

FIGURE 2. Einthoven limb leads and Einthoven triangle. Φ_L and Φ_R are, respectively, the potentials at the left and right arms, and Φ_F is the potential at the left leg [19].

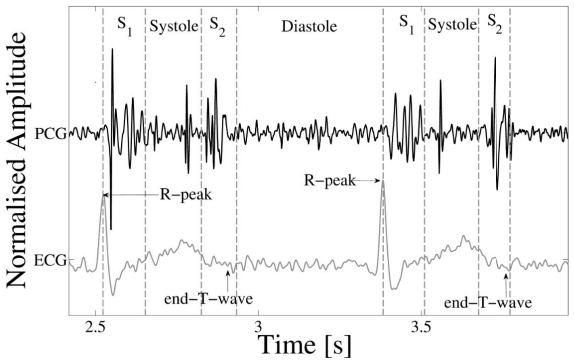

FIGURE 3. Synchronization between PCG and ECG, with R-peaks and end-T-waves of the ECG and segmentation of the fundamental heart sounds in the PCG [21].

useful for the diagnosis of cardiovascular diseases and for continuous monitoring of the heart rate and rhythm [13].

Numerous studies have firmly established the clinical ECG as a standard procedure. ECG acquisition in clinical practice is done using the 12-lead ECG system, which consists of three limb leads and three augmented leads (that record the electrical signals in the frontal plane), and six precordial leads (that record the electrical signals in the horizontal plane) [16]. Even though the 12-lead system has some redundancy [13], using several leads provides a view of the cardiac electrical activity from different perspectives, and also increases the probability of obtaining a good acquisition for diagnosis [12].

Single-lead ECGs have been increasingly used for monitoring cardiac arrhythmias in both clinical and non-clinical environments, and can be recorded using handheld devices that are widely available for both doctors and patients [17]. Even though these signals do not carry as much information as the 12-lead ECG system, they are a proven alternative for screening purposes. The exam is less time-consuming and can even be done by patients in their homes, removing accessibility barriers. It also alleviates some of the logistical challenges of doing an ECG exam in primary care, improving the early diagnosis of arrhythmias and other cardiac abnormalities [18].

A single-lead ECG acquired with an electronic stethoscope is typically measured on the patient's chest, which is in the frontal anatomical plane. This is the same plane where the bipolar Einthoven limb leads are measured (Fig. 2). This lead system is based on the assumption that the cardiac sources are represented by a dipole $\bar{p}$ located at the center of a homogeneous sphere representing the torso (the center of the equilateral Einthoven triangle). Thus, the voltages measured by the three limb leads are proportional to the projections of the electric heart vector on the sides of the lead vector triangle [19]. Considering this, we have:

$$V_I = p\cos(\alpha) = p_y \tag{1}$$

$$V_{II} = \frac{p}{2}\cos(\alpha) - \frac{\sqrt{3}}{2}\sin\alpha = 0.5p_y - 0.87p_z \tag{2}$$

$$V_{III} = -\frac{p}{2}\cos(\alpha) - \frac{\sqrt{3}}{2}p\sin(\alpha) = -0.5p_y - 0.87p_z \tag{3}$$

and we can verify that Kirchhoff 's voltage law is satisfied:

$$V_I + V_{III} = \frac{p}{2}\cos(\alpha) - \frac{\sqrt{3}}{2}\sin\alpha = V_{II} \tag{4}$$

Based on this assumption, we can conclude that only two leads are necessary to evaluate the heart's electrical activity in the frontal plane.

3) RELATING ECG AND PCG

The main features of the PCG and the ECG result from the same events in the cardiac cycle, and thus the two signals are time-locked with each other, as shown in Fig. 3. The QRS complex is directly related to the contraction of the ventricles, which seals the atrioventricular valves shut [13]. There is a slight delay between the electrical activation and mechanical contraction of the heart, and thus S1 occurs just after the QRS onset [20]. Ventricular systole ends with the closing of the semilunar valves, and this end of contraction is also marked by the T-wave [13]. S2 occurs approximately at the end of the T-wave.

Even though the two signals are synchronized, evidence of pathology in a PCG signal does not imply the existence of the same problems in the corresponding ECG [20]. For example, defective heart valves often cannot be detected from the ECG, but they manifest as heart murmurs and clicks in the PCG. In the same way, conduction disorders are easily detected in the ECG but are more difficult to identify using the heart sounds. Thus, combining the various features of the heart sounds with the ECG can provide a richer insight into the function of the heart and improve the diagnosis of heart disease.

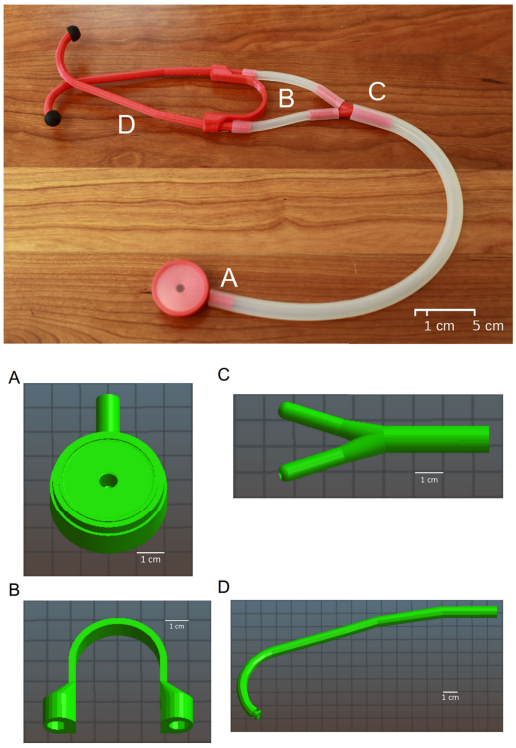

FIGURE 4. Glia stethoscope and digital models of 3D-printable parts. Image from [24].

The combination of the two signals can also enhance the segmentation of the PCG into the various heart sounds. Through R-peak and T-wave detectors and prior information about state duration averages, the locations of S1 and S2 can be easily inferred even in low-quality PCG signals [21].

II. METHODS

A. OVERVIEW

A core aspect when combining ECG and PCG for disease diagnosis is the temporal synchronization of both signals. Previous work has found restrictions associated with retrofitting external sensors to existing digital stethoscopes [12], [22]. To gain more control over the construction and sensor integration, this work builds upon the Glia stethoscope to devise an end-to-end design of a novel electronic stethoscope, without significantly changing the standard form factor. The Glia stethoscope[1] is an open-source 3D-printed acoustic stethoscope that is research-validated to operate as well as a Littmann Cardiology III, considered a gold-standard device [23].

A model of the original Glia stethoscope is presented in Fig. 4. It is composed of six different 3D printed parts: the stethoscope head (A), the ear tubes (D), the Y-piece which connects the head to the ear tubes (C), a spring (B), and a ring to attach the diaphragm to the head. Other hardware components include: a diaphragm that can be cut from standard PVC sheet material; standard earbuds; and three silicone tubes that can be purchased off-the-shelf to connect the stethoscope head to the Y-piece and the Y-piece to the ear tubes [24].

[1]https://github.com/GliaX/Stethoscope

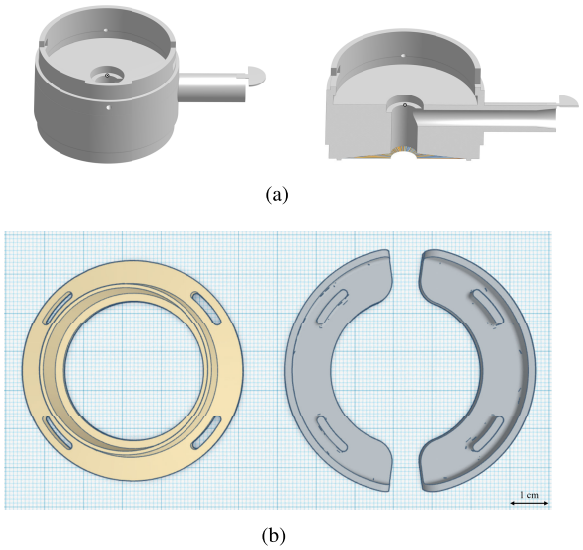

FIGURE 5. (a) Digital model of modified stethoscope head with hole for the electret microphone on the top. (b) Digital parts of the modified ring and the half-moon dry ECG electrodes.

This design was adapted to include phonocardiography and electrocardiography sensing capabilities, while keeping it low-cost and ensuring that the acoustic properties of the model weren't significantly altered. The form factor of the device was also considered so it could be used similarly to standard acoustic stethoscopes, with the same clinical procedure. As such, the stethoscope head was adapted to include PCG and ECG sensors, with 3D-printed polymer-based dry electrodes attached to the ring. In this work, we focus on the experimental characterization of the sensors and on evaluating the quality and morphology of the acquired biosignals.

B. FORM FACTOR

One of the main goals was preserving the standard analog auscultation feature of the stethoscope, to avoid creating barriers in the interaction between the end-user (the physician) and the device [22]. To integrate the PCG sensor, the stethoscope head was altered by adding a small hole in the back (Fig. 5(a)), with the same diameter as an electret microphone. Using this approach, the sound will still travel through the silicone tubes and ear pieces to be listened to by the doctor during the auscultation procedure, while simultaneously being recorded.

To allow ECG sensing capabilities, two 3D-printed dry electrodes with a half-moon shape were added to the side of the stethoscope head, attached to an altered ring (Fig. 5(b)). This design has several advantages, namely: 1) it doesn't alter the diaphragm of the original stethoscope, which is essential to ensure the quality and intensity of the sound reaching the

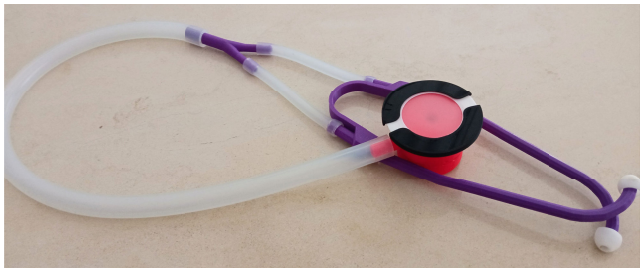

FIGURE 6. Photo of the developed device.

earpiece and the sensor microphone; 2) it provides a higher inter-electrode distance, which leads to a higher signal magnitude; 3) it enables a higher electrode conductance due to the increased surface area granted by the half-moon shape, which leads to higher SNR and reduced motion artifacts [25]; and 4) it leads to better ergonomics, since, by fitting the electrodes along the ring, the shape of the standard stethoscope is not modified.

The modified stethoscope parts (ring and stethoscope head) were printed using PLA (PolyLactic Acid) filaments. For the ECG dry electrodes, the electrical conductivity of the material also had to be considered, and as such we chose Protopasta Conductive PLA (ProtoPlant, Inc), which combines PLA with carbon black. It can be used on most PLA-compatible printers and has a resistivity of 30 Ω·cm along the Y-axis and 115 Ω·cm along the Z-axis. The electrical interface between the electrodes and the ECG sensor was done by fusing each wire to the material with heat, which has been tested and validated in [26]. The final device is presented in Fig. 6.

C. INSTRUMENTATION

The ScientISST SENSE[2] acquisition system was used for data acquisition and Bluetooth wireless streaming. This system is based on the ESP32 microcontroller and was coupled with two sensors, one for each signal modality (Fig. 7):

- A ScientISST ECG sensor [27], which has already been validated in previous studies [28]. It has a gain of 1100 and implements a bandpass filter with a high-pass (f_L) cut-off frequency of 0.5 Hz, and a low-pass (f_H) cut-off frequency of 40 Hz (the typical bandwidth for the analysis of the signal in monitoring applications [29]). It was used with a virtual ground configuration to measure a single-lead ECG.
- A PCG sensor based on an audio amplification circuit that uses an electret microphone with a frequency response between 20 Hz and 16000 Hz, 2.2 kΩ impedance, 60 Hz SNR, and -40 dB sensitivity. It is coupled with an LM4861 amplifier, with a gain of 40, a high-pass (f_L) cut-off frequency of approximately 21 Hz, and a low-pass (f_H) cut-off frequency of approximately 408 Hz (which were chosen based on the frequency content of the heart sounds [30]).

[2]https://www.scientisst.com/sense

TABLE 1. Main characteristics of the population. Categorical variables are expressed as frequencies and percentages and continuous variables as mean ± standard deviation.

Variables		n=21
Age group	18-24	15 (71.4%)
	25-34	5 (23.8%)
	65+	1 (4.8%)
Sex	Male	12 (57.1%)
	Female	9 (42.9%)
Height (cm)		170.2 ± 9.2
Weight (kg)		63.3 ± 11.8

The ScientISST SENSE Web App,[3] which allows simultaneous visualization and recording of the data streamed by the device, was used to record the data on a base station.

Multimodal signals were collected from 21 volunteers. The main characteristics of the population are described in Table 1; it is important to highlight that one participant had a previous diagnosis of a heart murmur. Initially, the relevant demographic and clinical history data were collected, and after that, a simultaneous phonocardiogram and electrocardiogram were recorded using the proposed device. The auscultations were performed with the subjects seated and at rest, with the stethoscope placed approximately on the third left intercostal space. Both signals were acquired with a sampling frequency of 2000 Hz and an amplitude resolution of 12 bits. Python 3.8 and the scikit-learn [31] (version 1.0.1) and BioSPPy [32] (version 1.0.0) libraries were used for the data analysis.

This study was conducted in accordance with the Declaration of Helsinki and approved by the Ethics Committee of Instituto Superior Técnico (Statement n° 4/2023). Written consent was obtained for the participants prior to their enrollment, and all data were treated anonymously. Subjects who were under 18 years of age or who had any physical or mental inability to understand and accept the informed consent were excluded from the study.

III. RESULTS

A. ACOUSTIC TRANSFER

To verify that the modifications made to the stethoscope head did not significantly alter the acoustic properties of the stethoscope, the acoustic transfer of the new design was compared with the one of the original Glia stethoscope. Currently, there is no standard method to compare the acoustic properties of different stethoscopes, with most evaluations being based on subjective opinions and agreement between users. More objective methods typically use a phantom to simulate the vibrations of the chest and have the advantage of being easier to replicate for independent validations [24].

[3]https://sense.scientisst.com

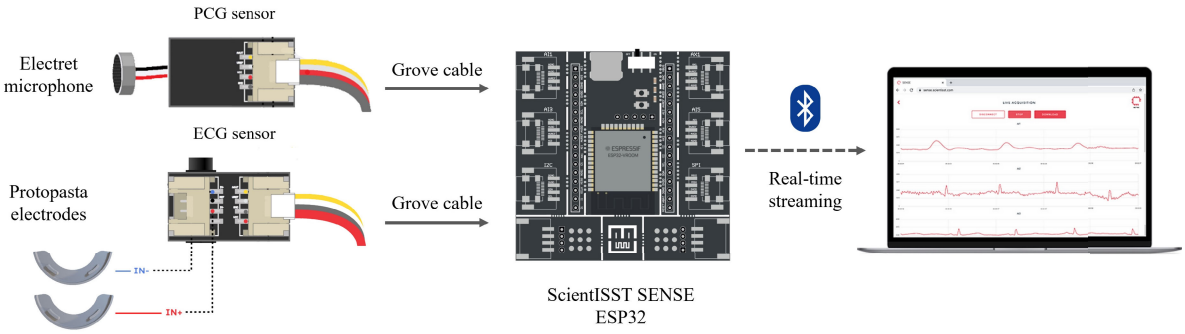

FIGURE 7. Simplified diagram of system architecture.

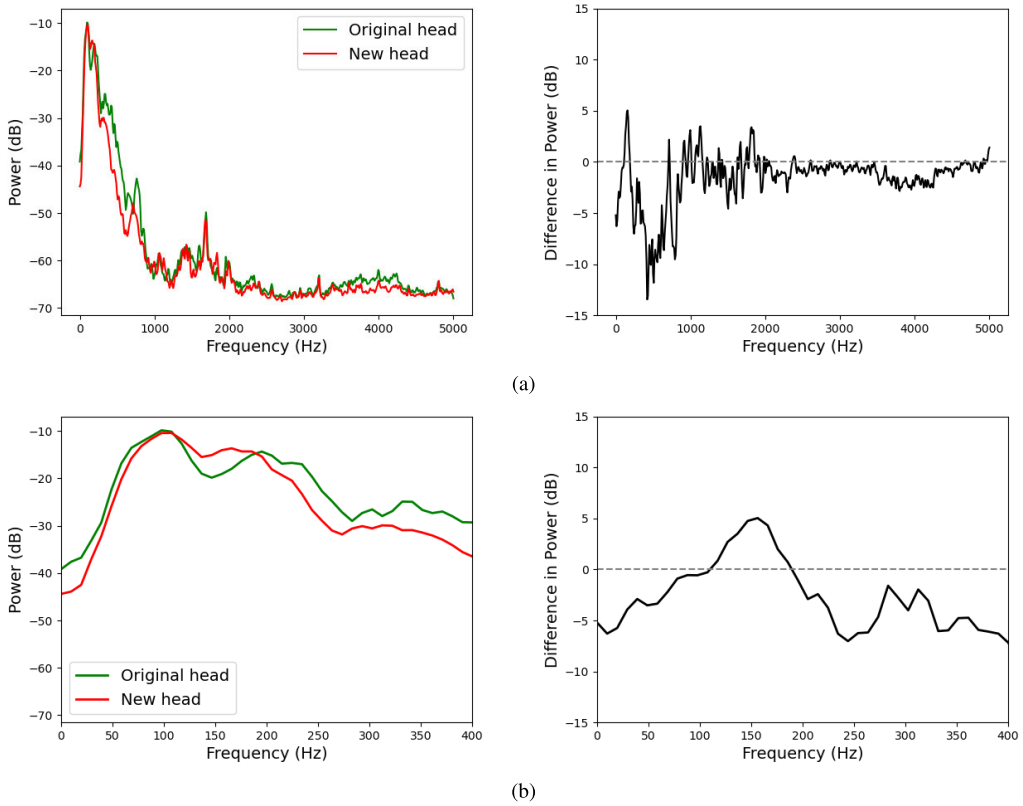

FIGURE 8. Stethoscope output frequency responses of the Glia stethoscope with the original head and of the developed device with the modified head, (a) for the full frequency spectrum and (b) for the frequencies of interest in PCG signals. The decibel difference in power corresponds to the new device minus the original. The magnitude spectra were calculated by applying the Fast Fourier Transform (FFT) to segments of the signal with a Blackman-Harris window of size 1024 and then averaging the segments together.

We adopted the same experimental setup that was used to compare the frequency response of the Glia stethoscope with the one of the Littmann Cardiology III, described in [24]. A latex balloon was filled with 2L of water and used as a phantom, to which both our proposed electronic stethoscope with the altered head and the original Glia stethoscope were applied. The phantom excitations were done by an external speaker (Adam Audio T5V nearfield monitor) which was in contact with the balloon, and white noise with frequencies between 0 and 5000 Hz (generated with Audacity® 3.1.3) was played for 15 seconds. The output of the stethoscopes was recorded by a microphone placed at the end of the silicone tubes that connect the stethoscope head to the earpieces.

This experiment was repeated three times, and the average frequency responses are presented in Fig. 8, demonstrating that the proposed device performed similarly to the Glia stethoscope. In the frequencies of interest for the analysis of PCG signals, between 25 and 400 Hz [30], the devices exhibit similar behavior, emphasizing the lower frequency regions

TABLE 2. Average heart rates (HR) calculated from ECG and PCG and average absolute differences in Beats Per Minute (bpm) of all signals with and without outliers.

	ECG HR	PCG HR	Absolute HR Difference
With outliers	82.1±12.1	83.0±12.2	2.1±3.8
Without outliers	82.1±12.4	82.2±11.9	1.3±1.8

between 50 and 200 Hz, with a slight roll-off in the higher frequencies.

B. HEART RATE AND AUSCULTATION POINTS

An example of unfiltered ECG and PCG signals acquired simultaneously with the device can be seen in Fig. 9. It is possible to identify the main fiducial points and structures and verify their alignment: the S1 sound occurs immediately after the R-peak and the S2 sound occurs immediately after the end of the T-wave. The PCG was segmented based on ECG fiducials and the heart sound states duration averages derived in [30].

Before further analysis, all signals were filtered using a FIR filter with order equal to half of the sampling frequency, using cutoff frequencies of 0.5 and 40 Hz for the ECG and 25 and 400 Hz for the PCG.

To evaluate the concurrence between the multimodal signals in all the subjects, we compared the average heart rates obtained from each signal. For the ECG, the average number of beats per minute was calculated by counting the number of R peaks (using the segmentation algorithm described in [33]) in the whole signal duration. For the PCG, the heart rate was calculated by counting the number of S1 heart sounds in the whole signal duration (after segmenting the signal with a recurrent neural network).

Table 2 and Fig. 10 show a comparison of the heart rates calculated for both signals. The scatter and Bland-Altman plots (Fig. 10(a) and 10(b)) show that there is a high agreement between the two measurements for all the samples, with the exception of an outlier (marked in red), which corresponds to a sample where the PCG signal was highly corrupted by noise (Fig. 10(c)). This is common in heart sound signals since ambient speech, motion artifacts, and other physiological sounds all contribute with in-band noise that is difficult to remove. In these cases, the simultaneous ECG signal is essential to identify and segment the heart sounds.

In Fig. 11 an example of ECG and PCG signals acquired at the different auscultation points is shown. Both signals have good quality, and the main fiducial points can be clearly identified. S1 and S2 are present in all PCG signals, as expected, but depending on the area of the chest and its closeness to each heart valve, the stethoscope amplifies the cardiac sounds differently.

As the stethoscope head is placed on the different auscultation points, we will also be looking at the heart's electrical axis from different perspectives and, as such, there is a high variation in the morphology of the recorded ECG waves. If we rotate the stethoscope head on the same auscultation point the effect on the ECG will be similar, since, by changing the electrodes' position, the heart's electrical activity will be recorded from a different perspective.

C. ECG LEADS CHARACTERIZATION

Since the ECG leads acquired with the stethoscope are bipolar and measured in the frontal plane, we can assume that they follow the same properties of the Einthoven lead system. Eight signals were collected from one subject by rotating the stethoscope head counterclockwise in increments of 45° (Fig. 12), always on the same auscultation point in the third left intercostal space. If these ECG leads obtained at different rotations also follow Kirchhoff's law we have, for example:

$$V_{0^\circ} = p\cos(\alpha) = p_y \tag{5}$$

$$V_{90^\circ} = p\sin(\alpha) = p_z \tag{6}$$

$$V_{45^\circ} = \frac{\sqrt{2}}{2}p\cos(\alpha) + \frac{\sqrt{2}}{2}p\sin(\alpha) = \frac{\sqrt{2}}{2}(V_{0^\circ} + V_{90^\circ}) \tag{7}$$

To verify this, the heartbeat waveform morphologies of the different leads were compared by segmenting the ECG signals into individual beats and then evaluating the correlation between the heartbeat waveforms of the experimental leads at different rotation angles and the equivalent beats obtained through Kirchhoff's law (from the adjacent ECG leads, at ± 45°). The comparison between the ECG beats was done with Pearson's Correlation Coefficient [34] (Eq. (8)):

$$\text{PCC} = \frac{\sum_{i=1}^{n}(x_i - \bar{x})(y_i - \bar{y})}{\sqrt{\sum_{i=1}^{n}(x_i - \bar{x})^2(y_i - \bar{y})^2}} \tag{8}$$

The outlier beats were removed by applying the DBSCAN algorithm with the cosine distance metric [35]. The results are presented in Table 3 and are in accordance with what can be observed in Fig. 13. All the leads have a very high correlation, except for the ones obtained at rotation angles of 45° and 225°, which have low correlation coefficients. A possible explanation is the fact that these signals have a very low amplitude, making them more sensitive to small errors in the angle of rotation of the stethoscope.

This shows that the ECG leads measured with the stethoscope follow Kirchhoff's law, similarly to the Einthoven leads. Thus, to evaluate all the frontal plane components of the heart's electrical activity we only need to perform two acquisitions on the same auscultation point with the stethoscope head at different angles. As a result, the proposed stethoscope design was further enhanced by including two additional dry ECG electrodes perpendicular to the ones of the original design (Section II), to allow the recording of two different ECG leads at the same time.

Each half-moon electrode part was split into two separate electrodes, for a total of four electrodes on the stethoscope

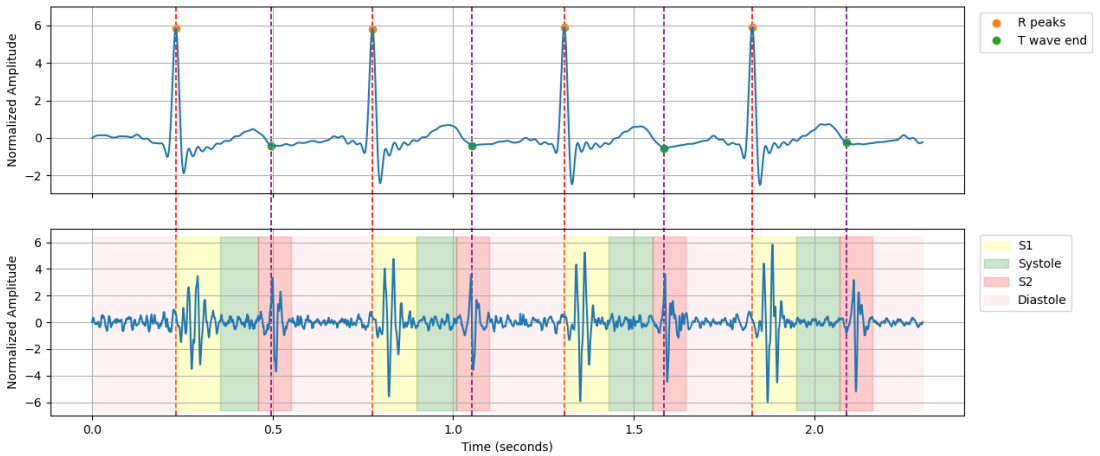

FIGURE 9. Example ECG and PCG signals acquired with the device. The PCG is segmented into the fundamental heart sound states, which are aligned with the R-peak and end T-wave positions of the ECG.

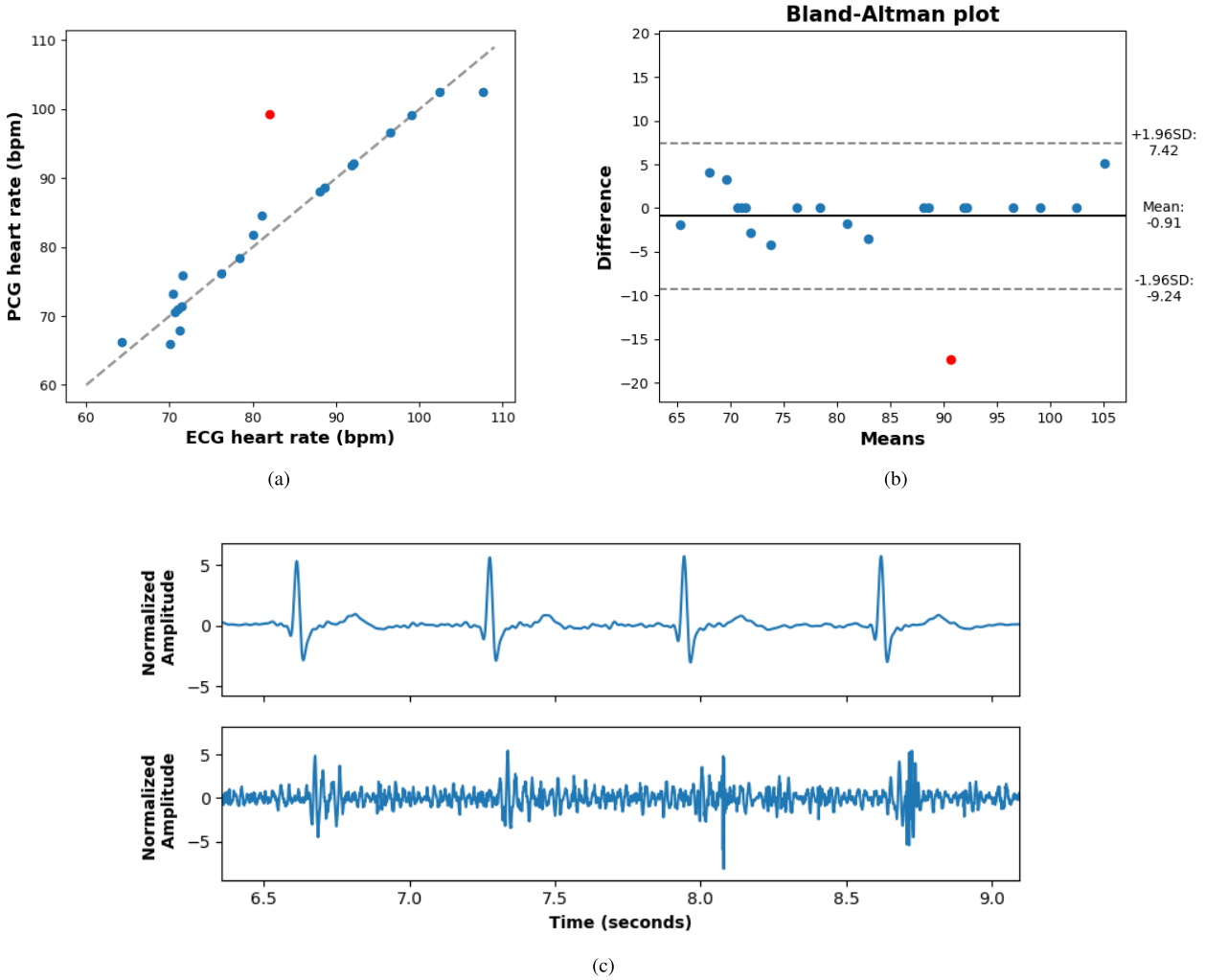

FIGURE 10. (a) Scatter plot comparing ECG and PCG average heart rates. The dashed line represents an equal heart rate in both signals. (b) Bland-Altman plot showing the agreement between heart rates calculated for the ECG and PCG, with 95% limits of agreement. Outliers are shown in red. (c) Signal segment of outlier sample with noisy PCG signal.

head. The positive electrodes were placed at the left and bottom sides (Fig. 14). Four acquisitions were performed on the same subject by rotating the stethoscope head counter-clockwise at the angles of 0°, 45°, 180°, and 225°. Since

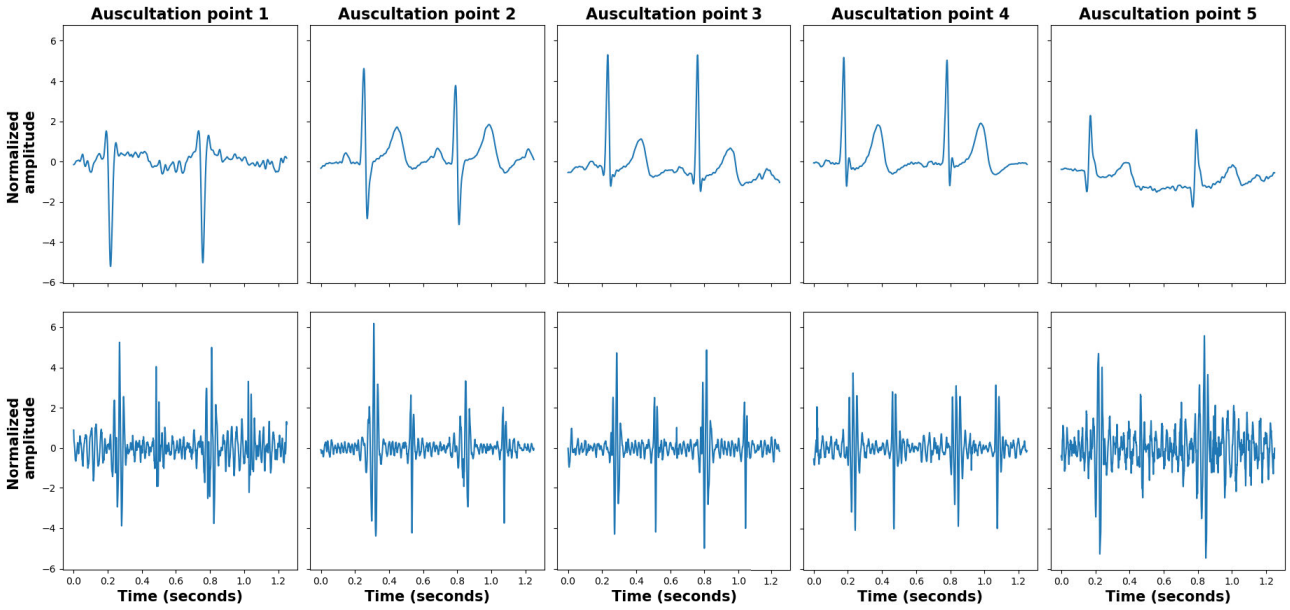

FIGURE 11. Example of ECG and PCG signals acquired with the stethoscope head at the different auscultation points.

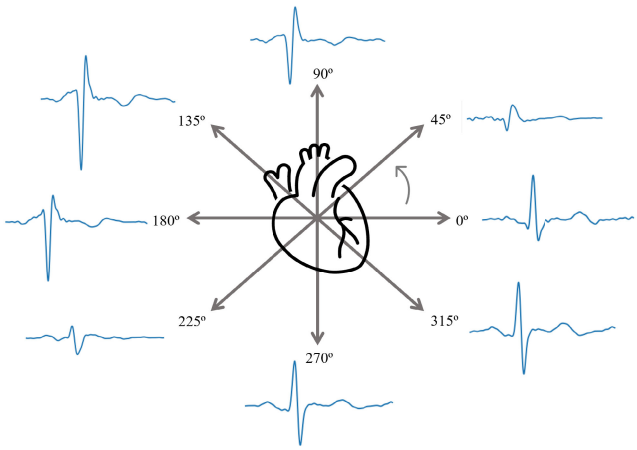

FIGURE 12. ECG waveforms of leads measured at different angles of rotation of the stethoscope head, relative to the frontal plane.

TABLE 3. Pearson's correlation coefficient between heartbeat waveforms of experimental singe-lead ECGs at different rotation angles and the equivalent waveforms obtained through Kirchhoff's law (from the adjacent ECG leads, at ± 45°).

Angle	Pearson's Correlation Coefficient
0º	0.952±0.019
45º	0.427±0.226
90º	0.977±0.011
135º	0.992±0.005
180º	0.970±0.015
225º	0.289±0.195
270º	0.987±0.006
315º	0.993±0.004

there are two perpendicular ECG leads, these measurements correspond to a total of eight signals that span all the angles of rotation represented in Fig. 12.

The previous analysis was repeated for the two-lead ECG case. The results of Table 4 and Fig. 15 show that the calculated waveforms have a high correlation with the experimental measurements, showcasing that by integrating two ECG sensors on the stethoscope head for 2-lead ECG acquisition it is possible to estimate additional leads at any angle, and thus obtain a full view of the heart's electrical activity in the frontal plane.

D. COMPARISON OF ECG LEADS WITH LEAD I

The beat waveforms of the ECG leads obtained at different rotations were also compared with the ones of the standard Lead I, which was acquired simultaneously. This comparison was done using the same method as in Section III-C: the ECGs were segmented into individual beats and, after outlier removal, Pearson's correlation coefficient was calculated for each pair of leads. All the rotation angles had a high correlation with the Lead I channel, as presented in Table 5.

Surprisingly, the leads with the highest correlation were the ones obtained in the vertical axis at 270° and 90°, instead of the ones obtained in the same direction as Lead I, in the horizontal axis. This can also be verified in Fig. 16. A possible explanation is that the lead vectors created by the electrodes of the device (which are placed at a short distance from each other on the chest) do not span the same volume as the electrodes of Lead I (which are placed on the right and left

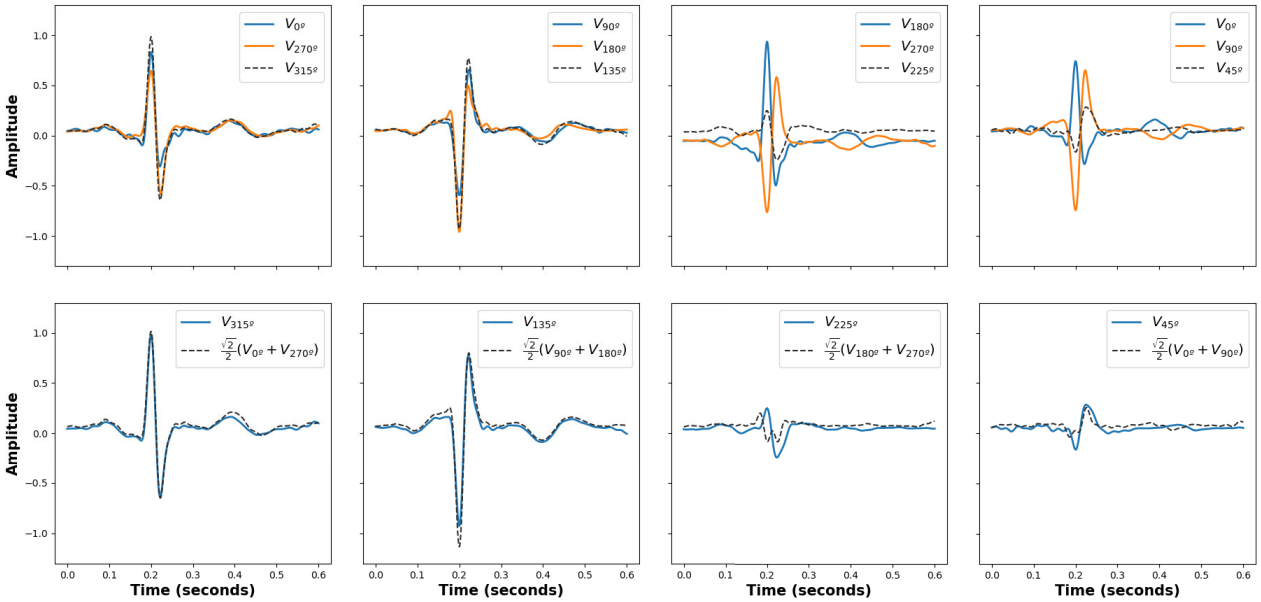

FIGURE 13. Example of heartbeat waveforms of experimental leads measured at different rotation angles and the equivalent waveforms obtained through Kirchhoff's law (from the adjacent ECG leads, at ± 45°).

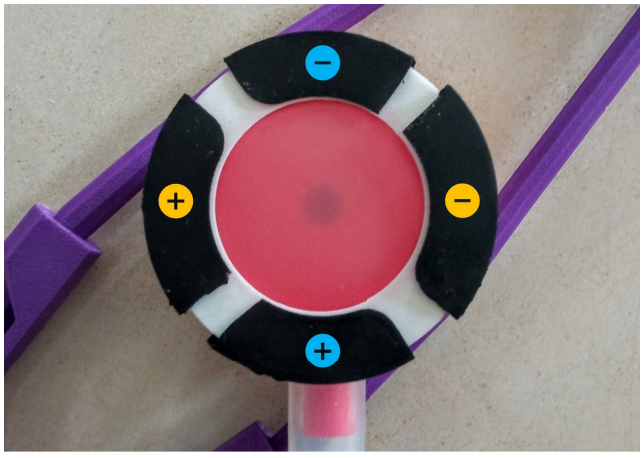

FIGURE 14. Disposition and polarity of two pairs of ECG dry electrodes on the stethoscope head, for the acquisition of two ECG leads. The electrodes with positive polarity are on the bottom and left sides.

TABLE 4. Pearson's correlation coefficient between heartbeat waveforms of experimental 2-lead ECGs at different rotation angles and the equivalent waveforms obtained through Kirchhoff's law (from the adjacent two-lead ECG pair).

Angle	Pearson's Correlation Coefficient
0º	0.959±0.011
45º	0.169±0.108
90º	0.952±0.015
135º	0.994±0.002
180º	0.967±0.004
225º	0.372±0.083
270º	0.990±0.003
315º	0.988±0.003

arms). The projections of the electric heart vector on the lead vector will therefore be different, altering the morphology of the measured ECG signals. Nonetheless, this high correlation suggests that the ECG leads measured with the proposed device are clinically meaningful.

IV. DISCUSSION

Our results show that the PCG and ECG are adequately acquired and that both signals have a different morphology depending on the point of auscultation, as expected.

Since the electrodes are fixed to the stethoscope head, the recorded ECG will have a different morphology depending on the device's rotation. As a result, an important contribution of this work is the experimental evaluation of the relationships between the leads obtained at different angles. They all have a high correlation with Lead I (with the highest correlation for the leads acquired along the vertical axis, at 270° and 90°), suggesting that they all contain meaningful information for CVD screening.

It was also found that the ECG leads measured with the stethoscope follow Kirchhoff's law, similarly to the Einthoven leads, meaning that to evaluate all the frontal plane components of the heart's electrical activity we only need to perform two acquisitions in the same auscultation point with the stethoscope head at different angles. By recording two ECG leads simultaneously (with the original electrodes split

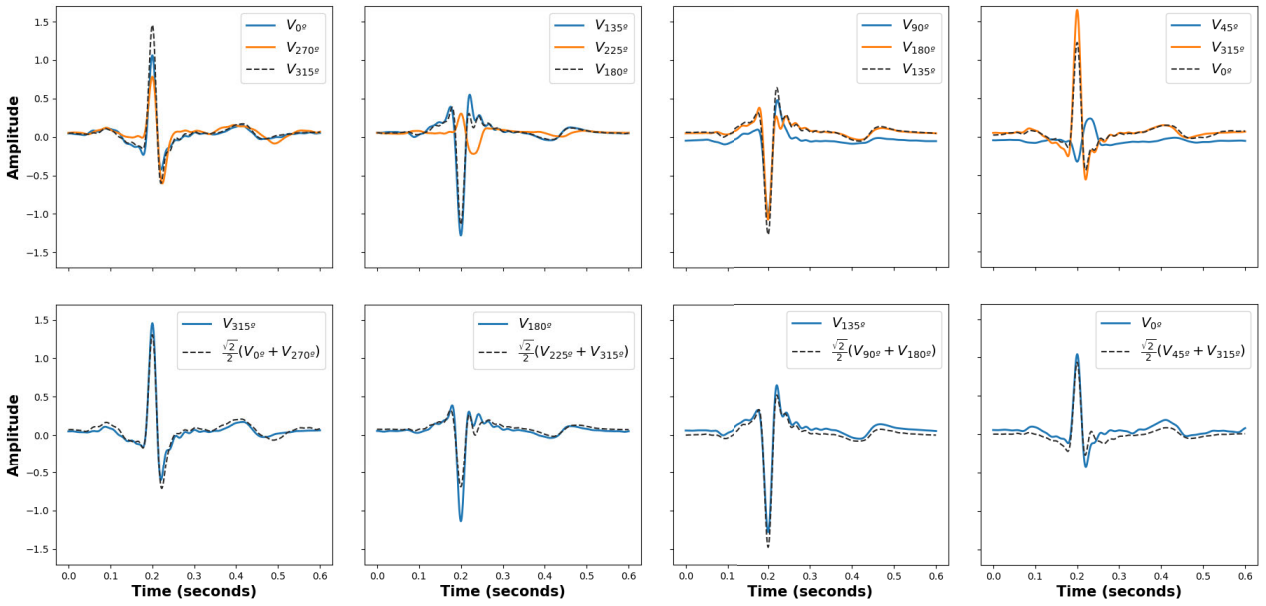

FIGURE 15. Example of heartbeat waveforms of experimental leads measured at different rotation angles and the equivalent waveforms obtained through Kirchhoff's law (from the adjacent two lead ECG pair).

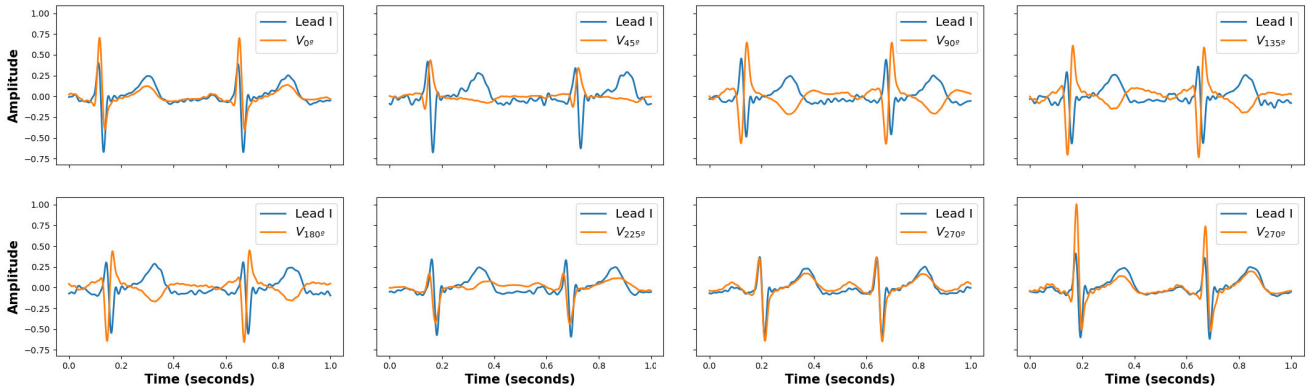

FIGURE 16. One second segments of ECGs acquired with experimental leads at different angles and with the standard Lead I electrode positioning.

TABLE 5. Pearson's correlation coefficient between heartbeat waveforms of reference Lead I channel and experimental leads at different rotation angles.

Angle	PCC
0º	0.829±0.089
45º	-0.847±0.020
90º	**-0.911±0.017**
135º	-0.877±0.017
180º	-0.862±0.015
225º	0.789±0.096
270º	**0.916±0.008**
315º	0.856±0.014

in two), we verified that it is possible to calculate additional ECG leads in the frontal plane from just one measurement.

This preliminary evaluation resulted in a new approach to ECG acquisition during auscultation, with more than one lead. By using this design with four electrodes on a standard auscultation procedure (through the five auscultation points), it is possible to record 10 ECG leads that provide a view of the electrical activity of the heart from different perspectives and 5 PCG signals that reflect the function of the different heart valves. This provides a high amount of additional information without altering the clinical routine.

V. CONCLUSION

Cardiac auscultation is the most common and cost-effective screening tool for CVDs. However, it is still mostly done with acoustic stethoscopes, which, despite their simplicity, have the disadvantage of needing to be operated by trained health professionals with enough clinical experience to master this skill. Electronic stethoscopes and automatic decision systems

for disease screening could significantly speed up treatment and referrals, improving the patient's outcome [4]. Combining ECG and PCG acquisition in the same device enables us to simultaneously inspect the electrical and mechanical condition of the heart, further improving the accuracy of the heart disease diagnosis.

Our approach overcomes the limitations of current devices by incorporating ECG and PCG sensors in an acoustic stethoscope without significantly altering its form factor or acoustic transfer properties, facilitating its integration into clinical practice. The inclusion of two ECG sensors to record simultaneous leads at a known angle is also a novelty compared to the commercially available alternatives. Furthermore, the device is based on open-source components, which makes it more accessible and easily upgradeable. The ability to collaborate, share the technology, and save the acquired signals for further analysis could make it an important tool in both research and education, where access to these technologies is often difficult.

The initial evaluation demonstrated promising results for further development. The next step is a full, comprehensive evaluation of the prototype in a real-world clinical setting, with healthy subjects and patients with diagnosed cardiovascular pathologies. It is especially important to do this evaluation in comparison with standard medical tools for cardiac monitoring (such as the 12-lead ECG), in order to validate its clinical usefulness. Future research should also focus on exploring the integration of this form factor into other brand-name stethoscopes (such as the Littmann Classic or Littmann Cardiology), which could facilitate the acceptability of the device by health professionals.

The low-cost, portability, and simplicity of the device, allied with computer-aided techniques for automatic diagnosis, could significantly facilitate the early screening of CVD. We believe this system would have the highest impact in primary care facilities as part of the auscultation routine, in telemedicine, or areas with difficult access to an integrated health system. In the latter case, an automatic screening tool that is not dependent on trained professionals could significantly reduce the mortality and morbidity associated with both congenital and acquired cardiopathies.

REFERENCES

[1] WHO. *Cardiovascular Diseases (CVD)*. Accessed: Aug. 22, 2022. [Online]. Available: https://www.who.int/news-room/fact-sheets/detail/cardiovascular-diseases-(cvds)

[2] M. E. H. Chowdhury, A. Khandakar, K. Alzoubi, S. Mansoor, A. M. Tahir, M. B. I. Reaz, and N. Al-Emadi, "Real-time smart-digital stethoscope system for heart diseases monitoring," *Sensors*, vol. 19, no. 12, p. 2781, Jun. 2019, doi: 10.3390/s19122781.

[3] S. Leng, R. S. Tan, K. T. C. Chai, C. Wang, D. Ghista, and L. Zhong, "The electronic stethoscope," *Biomed. Eng. OnLine*, vol. 14, no. 1, pp. 1–37, Dec. 2015, doi: 10.1186/s12938-015-0056-y.

[4] J. Oliveira, F. Renna, P. D. Costa, M. Nogueira, C. Oliveira, C. Ferreira, A. Jorge, S. Mattos, T. Hatem, T. Tavares, A. Elola, A. B. Rad, R. Sameni, G. D. Clifford, and M. T. Coimbra, "The CirCor DigiScope dataset: From murmur detection to murmur classification," *IEEE J. Biomed. Health Informat.*, vol. 26, no. 6, pp. 2524–2535, Jun. 2022, doi: 10.1109/JBHI.2021.3137048.

[5] F. Renna, J. Oliveira, and M. T. Coimbra, "Deep convolutional neural networks for heart sound segmentation," *IEEE J. Biomed. Health Informat.*, vol. 23, no. 6, pp. 2435–2445, Nov. 2019, doi: 10.1109/JBHI.2019.2894222.

[6] W. Phanphaisarn, A. Roeksabutr, P. Wardkein, J. Koseeyaporn, and P. Yupapin, "Heart detection and diagnosis based on ECG and EPCG relationships," *Med. Devices*, vol. 4, pp. 133–144, Apr. 2011, doi: 10.2147/MDER.S23324.

[7] A. Kazemnejad, P. Gordany, and R. Sameni, "An open-access simultaneous electrocardiogram and phonocardiogram database," *bioRxiv*, May 2021, doi: 10.1101/2021.05.17.444563.

[8] C. Landgraf, P. Goolkasian, and T. Crouch, "Wireless cardiac sensor," U.S. Patent 0 256 061 A1, Sep. 13, 2018. [Online]. Available: https://patents.google.com/patent/US20180256061A1

[9] E Health. *Eko DUO ECG + Digital Stethoscope*. Accessed: 12, Sep. 2022. [Online]. Available: https://shop.ekohealth.com/products/duo-ecg-digital-stethoscope

[10] R. Kappor, "Mobile front-end system for comprehensive cardiac diagnosis," U.S. Patent 9 492 138 B2, Nov. 15, 2016. [Online]. Available: https://patents.google.com/patent/US9492138B2

[11] M. Engineering. *CardioSleeve—ECG & Heart Sound Stethoscope Add-On*. Accessed: Sep. 12, 2022. [Online]. Available: https://www.2mel.nl/projects/rijuven-cardiosleeve-ecg-heart-sound-stethoscope/

[12] M. Martins, P. Gomes, C. Oliveira, M. Coimbra, and H. P. Silva, "Design and evaluation of a diaphragm for electrocardiography in electronic stethoscopes," *IEEE Trans. Biomed. Eng.*, vol. 67, no. 2, pp. 391–398, Feb. 2020, doi: 10.1109/TBME.2019.2913913.

[13] R. M. Rangayyan, *Biomedical Signal Analysis*, 2nd ed. Piscataway, NJ, USA: IEEE Press, 2015, pp. 21–74.

[14] M. C. Kusko and K. Maselli, *Introduction to Cardiac Auscultation*. London, U.K.: Springer, 2015, pp. 3–14, doi: 10.1007/978-1-4471-6738-9_1.

[15] M. Waqar, S. Inam, M. A. U. Rehman, M. Ishaq, M. Afzal, N. Tariq, and F. Amin, "Arduino based cost-effective design and development of a digital stethoscope," in *Proc. 15th Int. Conf. Emerg. Technol. (ICET)*, Dec. 2019, pp. 1–6, doi: 10.1109/ICET48972.2019.8994674.

[16] P. Podrid, R. Malhotra, R. Kakkar, P. A. Noseworthy, H. J. Wellens, and R. Desanctis, *Podrid's Real-World ECGs: The Basics: A Master's Approach to the Art and Practice of Clinical ECG Interpretation*, vol. 1. Minneapolis, MN, USA: Cardiotext Publishing, 2012, pp. 1–18.

[17] M. P. Witvliet, E. P. M. Karregat, J. C. L. Himmelreich, J. S. S. G. de Jong, W. A. M. Lucassen, and R. E. Harskamp, "Usefulness, pitfalls and interpretation of handheld single-lead electrocardiograms," *J. Electrocardiology*, vol. 66, pp. 33–37, May 2021, doi: 10.1016/j.jelectrocard.2021.02.011.

[18] E. P. M. Karregat, J. C. L. Himmelreich, W. A. M. Lucassen, W. B. Busschers, H. C. P. M. van Weert, and R. E. Harskamp, "Evaluation of general practitioners' single-lead electrocardiogram interpretation skills: A case-vignette study," *Family Pract.*, vol. 38, no. 2, pp. 70–75, Mar. 2021.

[19] J. Malmivuo and R. Plonsey, *Bioelectromagnetism Principles and Applications of Bioelectric and Biomagnetic Fields*. New York, NY, USA: Oxford Univ. Press, 1995.

[20] F. Safara, S. Doraisamy, A. Azman, A. Jantan, and A. R. A. Ramaiah, "Multi-level basis selection of wavelet packet decomposition tree for heart sound classification," *Comput. Biol. Med.*, vol. 43, no. 10, pp. 1407–1414, Oct. 2013, doi: 10.1016/j.compbiomed.2013.06.016.

[21] D. B. Springer, L. Tarassenko, and G. D. Clifford, "Logistic regression-HSMM-based heart sound segmentation," *IEEE Trans. Biomed. Eng.*, vol. 63, no. 4, pp. 822–832, Apr. 2016, doi: 10.1109/TBME.2015.2475278.

[22] R. Baptista, H. Silva, and M. Rocha, "Design and development of a digital stethoscope encapsulation for simultaneous acquisition of phonocardiography and electrocardiography signals: The SmartHeart case study," *J. Med. Eng. Technol.*, vol. 44, no. 4, pp. 153–161, May 2020, doi: 10.1080/03091902.2020.1757770.

[23] Glia. *Stethoscope*. Accessed: 14, Sep. 2022. [Online]. Available: https://glia.org/pages/stethoscope

[24] A. Pavlosky, J. Glauche, S. Chambers, M. Al-Alawi, K. Yanev, and T. Loubani, "Validation of an effective, low cost, free/open access 3D-printed stethoscope," *PLoS ONE*, vol. 13, no. 3, pp. 1–10, 2018, doi: 10.1371/journal.pone.0193087.

[25] E.-R. Symeonidou, A. D. Nordin, W. D. Hairston, and D. P. Ferris, "Effects of cable sway, electrode surface area, and electrode mass on electroencephalography signal quality during motion," *Sensors*, vol. 18, no. 4, p. 1073, 2018. [Online]. Available: https://www.mdpi.com/1424-8220/18/4/1073

[26] A. D. S. Silva, H. Almeida, H. P. da Silva, and A. Oliveira, "Design and evaluation of a novel approach to invisible electrocardiography (ECG) in sanitary facilities using polymeric electrodes," *Sci. Rep.*, vol. 11, no. 1, p. 6222, Mar. 2021.
[27] H. P. D. Silva, J. Guerreiro, A. Lourenço, A. Fred, and R. Martins, "BITalino: A novel hardware framework for physiological computing," in *Proc. Int. Conf. Physiological Comput. Syst.*, Jan. 2014, pp. 246–253.
[28] D. Batista, H. P. D. Silva, A. Fred, C. Moreira, M. Reis, and H. A. Ferreira, "Benchmarking of the BITalino biomedical toolkit against an established gold standard," *Healthcare Technol. Lett.*, vol. 6, no. 2, pp. 32–36, Apr. 2019.
[29] D. Guldenring, D. D. Finlay, R. R. Bond, A. Kennedy, and J. McLaughlin, "The effects of 0.67 Hz high-pass filtering on the spatial QRS-T angle," in *Proc. Comput. Cardiology (CinC)*, Sep. 2017, pp. 1–4.
[30] S. E. Schmidt, C. Holst-Hansen, C. Graff, E. Toft, and J. J. Struijk, "Segmentation of heart sound recordings by a duration-dependent hidden Markov model," *Physiological Meas.*, vol. 31, no. 4, pp. 513–529, Apr. 2010, doi: 10.1088/0967-3334/31/4/004.
[31] F. Pedregosa, G. Varoquaux, A. Gramfort, V. Michel, B. Thirion, O. Grisel, M. Blondel, P. Prettenhofer, R. Weiss, V. Dubourg, J. Vanderplas, A. Passos, D. Cournapeau, M. Brucher, M. Perrot, and E. Duchesnay, "Scikit-learn: Machine learning in Python," *J. Mach. Learn. Res.*, vol. 12 no. 10, pp. 2825–2830, 2012.
[32] C. Carreiras, A. P. Alves, A. Lourenço, F. Canento, H. Silva, A. Fred. (2015). *BioSPPy: Biosignal Processing in Python*. [Online]. Available: https://github.com/scientisst/BioSPPy
[33] P. Hamilton, "Open source ECG analysis software documentation," E. P. Limited, Somerville, MA, USA, Tech. Rep., 2002.
[34] P. Di Lena and L. Margara, "Optimal global alignment of signals by maximization of Pearson correlation," *Inf. Process. Lett.*, vol. 110, no. 16, pp. 679–686, Jul. 2010, doi: 10.1016/j.ipl.2010.05.024.
[35] M. Ester, H.-P. Kriegel, J. Sander, and X. Xu, "A density-based algorithm for discovering clusters in large spatial databases with noise," in *Proc. Int. Conf. Knowl. Discovery Data Mining (KDD)*, 1996, pp. 226–231.

SOFIA M. MONTEIRO was born in Alverca, Portugal, in September 1998. She received the M.Sc. degree in biomedical engineering from Instituto Superior Técnico, Universidade de Lisboa, in 2022, where she worked with Instituto de Telecomunicacoes. She is currently a Researcher with the Cardiology Department, Lisbon School of Medicine, Universidade de Lisboa. Her research interests include biosignal processing, machine learning, and medical devices.

HUGO PLÁCIDO DA SILVA (Senior Member, IEEE) was born in Vila Franca de Xira, Portugal, in August 1979. He received the Ph.D. degree in electrical and computers engineering from the University of Lisbon, Lisbon, Portugal, in 2015. Since 2004, he has been a Researcher in IT with the Instituto de Telecomunicações. He has been a Professor with the Instituto Superior Técnico, since 2019, and the Co-Founder and the Chief Innovation Officer of PLUX—Wireless Biosignals S.A., since 2007. His research interests include biosignal research, system engineering, signal processing, and machine learning. His work has been distinguished with numerous academic and technical awards.